https://doi.org/10.2352/lim.2023.4.1.09

Performance considerations for ray tracing in gradient-index optics with symplectic numerical methods

Ben McKeon and Alexander V. Goncharov; Applied Optics Group, School of Natural Sciences, University of Galway, Ireland

Abstract

The primary objective of this paper is to demonstrate the utility of symplectic numerical techniques for ray tracing within gradient-index media. The relevant mathematics are explained in brief, deriving the optical Hamiltonian independently of the Lagrangian optical formalism before constructing a symplectic ray tracing algorithm. Numerical experiments with the Lüneburg and Maxwell fish-eye lenses compare the effectiveness of symplectic methods with standard numerical integration techniques, challenging the idea that the increased accuracy of higher-order numerical methods justifies their elevated computational cost. Further uses for symplectic ray tracing are also discussed.

Introduction

Symplectic ray tracing is born out of Hamiltonian optics, first described by William Rowan Hamilton in his 1828 paper *Theory of systems of rays* [13]. Indeed, Hamilton's formalism was then applied to dynamics more generally [12], where it is now a fundamental component of undergraduate courses in both classical and quantum mechanics [8, 9]. While several volumes have been published specifically on Hamiltonian optics [4, 24, 28], Hamilton's analysis is seldom exploited to its full potential, typically being neglected in favour of an equivalent Lagrangian framework, which has proven useful for ray tracing in gradient-index (GRIN) media [15, 20, 25].

Nonetheless, by adopting the Hamiltonian perspective, we may construct numerical techniques for ray tracing in GRIN media that are both accurate and computationally inexpensive. Since the calculation of ray trajectories in GRIN lenses typically requires the solution of a nonlinear partial differential equation which is only analytic in certain cases [19], symplectic numerical methods prove to be valuable tools for nonlinear ray tracing.

Unfortunately, a number of problems plague the literature examining applications of symplectic numerical techniques in optics. Often, notation tends to vary between authors, making the assimilation of results from disparate papers difficult. Moreover, these papers are usually mathematically dense, demanding some familiarity with group theory and differential geometry of the reader in order to be fully understood [1, 2].

This publication, by comparison, seeks to minimise the use of mathematics that may be unfamiliar to optical engineers by focusing on the tangible benefits of symplectic integration schemes rather than placing any undue emphasis on their more abstract characteristics. To this end, the mathematical preliminaries necessary for the construction of symplectic numerical techniques are provided before comparing their accuracy with a number of common nonsymplectic numerical methods. To the best of the author's knowledge, the first instance of benchmarking for symplectic algorithms when applied to ray tracing problems is also presented. The paper then concludes by suggesting applications for symplectic methods in optics and computer imaging.

An overview of Hamiltonian optics

Numerous treatments of Hamiltonian optics begin by deriving an optical Lagrangian as a consequence of Fermat's principle before performing a Legendre transform on this Lagrangian to obtain the associated optical Hamiltonian [14, 29, 30]. Here, we dispense with this procedure entirely, instead deriving the optical Hamiltonian directly from the eikonal equation [26]

$$\left(\frac{\partial S}{\partial x}\right)^2+\left(\frac{\partial S}{\partial y}\right)^2+\left(\frac{\partial S}{\partial z}\right)^2=n^2(x,y,z), \tag{1}$$

where $n(x,y,z)$ is the refractive index, and S is the optical path length, defined as $\mathrm{d}S=n\ \mathrm{d}s$, with $\mathrm{d}s=\sqrt{\mathrm{d}x^2+\mathrm{d}y^2+\mathrm{d}z^2}$ representing an infinitesimal change in the geometric path length. Following algebraic manipulation, we may cast the terms on the right-hand side of (1) in an alternative form:

$$\begin{aligned}
\frac{\partial S}{\partial x}&=n(x,y,z)\frac{\mathrm{d}x}{\sqrt{\mathrm{d}x^2+\mathrm{d}y^2+\mathrm{d}z^2}}=n(x,y,z)\frac{\mathrm{d}x}{\mathrm{d}s}\coloneqq p_x,\\
\frac{\partial S}{\partial y}&=n(x,y,z)\frac{\mathrm{d}y}{\sqrt{\mathrm{d}x^2+\mathrm{d}y^2+\mathrm{d}z^2}}=n(x,y,z)\frac{\mathrm{d}y}{\mathrm{d}s}\coloneqq p_y,\\
\frac{\partial S}{\partial z}&=n(x,y,z)\frac{\mathrm{d}z}{\sqrt{\mathrm{d}x^2+\mathrm{d}y^2+\mathrm{d}z^2}}=n(x,y,z)\frac{\mathrm{d}z}{\mathrm{d}s}\coloneqq p_z,
\end{aligned} \tag{2}$$

thereby providing us with definitions for the optical momenta p_x, p_y and p_z, so called due to their similarity to momentum in mechanics. Likewise, we find

$$\begin{aligned}
n(x,y,z)\frac{\mathrm{d}p_x}{\mathrm{d}s}&=\frac{\partial n(x,y,z)}{\partial x},\\
n(x,y,z)\frac{\mathrm{d}p_x}{\mathrm{d}s}&=\frac{\partial n(x,y,z)}{\partial y},\\
n(x,y,z)\frac{\mathrm{d}p_z}{\mathrm{d}s}&=\frac{\partial n(x,y,z)}{\partial z}.
\end{aligned} \tag{3}$$

By defining $\mathrm{d}t=\frac{\mathrm{d}s}{n}$, we reduce (1) from a partial differential equation to a system of ordinary differential equations

$$\begin{aligned}
\frac{\mathrm{d}x}{\mathrm{d}t}&=p_x, & \frac{\mathrm{d}p_x}{\mathrm{d}t}&=\frac{\partial n(x,y,z)}{\partial x},\\
\frac{\mathrm{d}y}{\mathrm{d}t}&=p_y, & \frac{\mathrm{d}p_y}{\mathrm{d}t}&=\frac{\partial n(x,y,z)}{\partial y},\\
\frac{\mathrm{d}z}{\mathrm{d}t}&=p_z, & \frac{\mathrm{d}p_z}{\mathrm{d}t}&=\frac{\partial n(x,y,z)}{\partial z}.
\end{aligned} \tag{4}$$

However, to avoid confusion, some caution is warranted. Although the parameter t is analogous to time in a dynamical system and is even referred to as time in existing literature [21, 27], it does not represent physical time. Nevertheless, by making this change of variables, the optical momenta simply become the

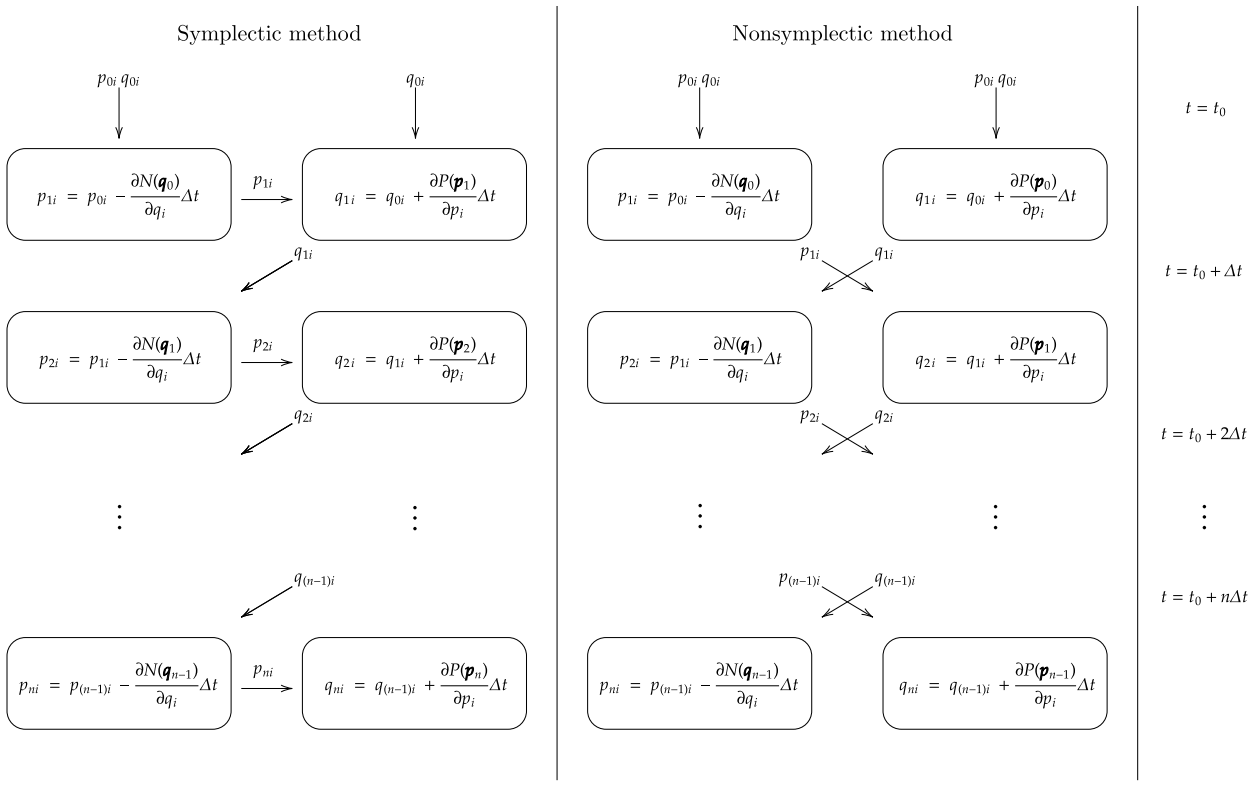

Figure 1. *Differences between symplectic and nonsymplectic methods. By using the momentum calculated during the same iteration to update the ray's position, symplectic methods typically return more accurate results.*

direction cosines for their respective axes. Moreover, by letting

$$\begin{aligned} p_x &= \frac{\partial H}{\partial p_x}, \quad \frac{\partial n(x,y,z)}{\partial x} = -\frac{\partial H}{\partial x}, \\ p_y &= \frac{\partial H}{\partial p_y}, \quad \frac{\partial n(x,y,z)}{\partial y} = -\frac{\partial H}{\partial y}, \\ p_z &= \frac{\partial H}{\partial p_z}, \quad \frac{\partial n(x,y,z)}{\partial z} = -\frac{\partial H}{\partial z}, \end{aligned} \tag{5}$$

we obtain Hamilton's equations. Solving the system in (5) then yields the requisite optical Hamiltonian

$$H = \frac{1}{2}\left(p_x^2 + p_y^2 + p_z^2 - n^2(x,y,z)\right). \tag{6}$$

Constructing a symplectic numerical method

The merits of Hamilton's formulation of geometric optics become more apparent by examining the dissimilarities in the behaviour of symplectic and nonsymplectic numerical methods. Figure 1 illustrates how a ray's position and optical momentum calculated during each iteration are handled differently by each method. A nonsymplectic method will update a ray's optical momentum and position using data obtained exclusively from the previous iteration, while a symplectic method initially calculates the ray's optical momentum, then, with this updated momentum, it obtains the ray's position during the same iteration. Hence, the error of a symplectic method remains bounded for a greater number of iterations when compared with an equivalent nonsymplectic method [6, 10, 11].

The application of symplectic methods to ray tracing in GRIN media is made possible by the fact that (6) is of the form $H = P(p_x, p_y, p_z) + N(x,y,z)$, making it separable. This allows the terms dependent on the ray's position and optical momentum to be treated independently. Symplectic numerical methods for separable Hamiltonians are constructed via splitting, giving two separate iterative schemes to calculate the position and optical momentum of a given ray. First, however, we rewrite Hamilton's equations in matrix form

$$\frac{\mathrm{d}\mathbf{z}}{\mathrm{d}t} = \{\mathbf{z}, H\}, \tag{7}$$

where $\mathbf{z} = (\mathbf{p}, \mathbf{q})$, $\mathbf{p} = (p_x, p_y, p_z)^T$, $\mathbf{q} = (x,y,z)^T$ and

$$\{\cdot, H\} = \sum_{i=1}^{k}\left(\frac{\partial \cdot}{\partial q_i}\frac{\partial H}{\partial p_i} - \frac{\partial \cdot}{\partial p_i}\frac{\partial H}{\partial q_i}\right) := D_H \cdot \tag{8}$$

is the Liouville operator [5]. It is now possible to express (7) as an ordinary differential equation $\dot{\mathbf{z}} = D_H \mathbf{z}$, whose solution is

$$\mathbf{z}(t) = \mathbf{z}(0)\exp(tD_H). \tag{9}$$

Recalling that (6) is separable, if we further define

$$\begin{aligned} \{\cdot, P\} &= \sum_{i=1}^{k}\left(\frac{\partial \cdot}{\partial q_i}\frac{\partial H}{\partial p_i}\right) := D_P \cdot, \\ \{\cdot, N\} &= -\sum_{i=1}^{k}\left(\frac{\partial \cdot}{\partial p_i}\frac{\partial H}{\partial q_i}\right) := D_N \cdot, \end{aligned} \tag{10}$$

we observe $D_H = D_P + D_N$. Expansion of the exponential yields

$$\exp\left[t(D_P + D_N)\right] = \prod_{i=1}^{m}\exp(tc_i D_P)\exp(td_i D_N) + O(t^{m+1}), \tag{11}$$

where $\sum_{i=1}^{m} c_i = \sum_{i=1}^{m} d_i = 1$ and m is the order of the symplectic method. From the definition of the matrix exponential, we write

$$\begin{aligned} \exp(tc_k D_P) &= \sum_{k=0}^{\infty} \frac{(tc_k D_P)^k}{k!}, \\ \exp(td_k D_N) &= \sum_{k=0}^{\infty} \frac{(td_k D_N)^k}{k!}. \end{aligned} \tag{12}$$

To eliminate the possibility of confusion with the imaginary unit, k replaces i as the index in (12). Performing a Taylor expansion with $m = 1$ then yields $d_k = c_k = 1$, i.e.

$$\begin{pmatrix} \exp(tc_k D_P) \\ \exp(td_k D_N) \end{pmatrix} \approx \begin{pmatrix} I + tD_P \\ I + tD_N \end{pmatrix} \tag{13}$$

Finally, multiplying the expansions in (13) by $\mathbf{z}_n = (\mathbf{p}_n, \mathbf{q}_n)$, we obtain the symplectic Euler method [11]

$$\begin{aligned} p_{i_{n+1}} &= p_{i_n} - \Delta t \frac{\partial N}{\partial q_i}(q_{i_n}), \\ q_{i_{n+1}} &= q_{i_n} + \Delta t \frac{\partial P}{\partial p_i}(p_{i_{n+1}}), \end{aligned} \tag{14}$$

where Δt is the step size between successive iterations. Similarly, higher-order symplectic methods can be constructed using fractional step sizes and by choosing appropriate values for c_i and d_i. However, finding the optimal values for these coefficients is often a tedious exercise in and of itself [7, 18, 31].

Results of numerical experiments

The Lüneburg lens

The Lüneburg lens is a radially symmetric, spherical lens capable of focusing incoming axially collimated rays to a single point on the lens' surface [16]. The majority of its applications to-date have been in the radio spectrum, such as a focusing element in radio telescopes and automotive radar [22, 23]. Recently, however, it has also seen increased use with visible light, being incoporated into silicon photonic devices [3, 32]. Its refractive index is given by

$$n(x,y) = \sqrt{2 - \frac{x^2+y^2}{R_0^2}}, \tag{15}$$

where R_0 is the radius of the lens and $0 \leq x^2 + y^2 \leq R_0^2$. Its optical Hamiltonian is therefore

$$H_{\text{Lüneburg}} = \frac{1}{2}\left(p_x^2 + p_y^2 + \frac{x^2+y^2}{R_0}\right) - 1. \tag{16}$$

Figure 2 depicts a ray trace through the Lüneburg lens, comparing the accuracy of first-, second-, and fourth order symplectic (symplectic Euler, velocity Verlet [10] and Ruth's method [7]) and nonsymplectic (Euler's method, RK2 and RK4) methods. The inset examines the behaviour of each method in detail as it approaches the focal point. The exact solution is also shown. The velocity Verlet method outperforms all other methods, indicating the use of a higher-order numerical integrator does not guarantee greater accuracy. The symplectic Euler method vastly outperforms its nonsymplectic counterpart, while differences in accuracy between symplectic and nonsymplectic methods seem to diminish with increasing order. Figure 3 further confirms these findings, containing the error of each method for various step sizes. Figure 4 presents the median computation time required to complete a ray trace for each method. Simulations were carried out using a Dell™ Inspiron 5570 computer with an Intel® Core™ i7 CPU and 8 GB DDR4 RAM running on battery power.

At larger step sizes, the symplectic Euler method appears noticeably faster than the standard Euler method, presumably as it does not need to store data from the previous iteration in memory to perform each subsequent iteration, though this advantage reduces with the step size. The second-order velocity Verlet and RK2 methods follow a similar trend, with Ruth's method being slower than RK4 by more than half an order of magnitude. While both fourth-order methods exhibiting a reduction in the required computation time once Δt is brought below 10^{-2}, further investigation is required to ascertain whether or not this unexpected trend persists with a greater number of trials.

Maxwell's fish-eye lens

The Maxwell fish-eye lens was first described by James Clerk Maxwell as a spherical lens capable of directing incident rays along circular arcs [17]. The refractive index required to produce such ray trajectories is described by

$$n(x,y) = n_0 \left(1 + \frac{x^2+y^2}{R_0^2}\right)^{-1}, \tag{17}$$

where R_0 is the lens radius with $0 \leq x^2 + y^2 \leq R_0^2$ as before and n_0 is the refractive index at the surface of the lens. Thus, the optical Hamiltonian for Maxwell's fish-eye is

$$H_{\text{Maxwell}} = \frac{1}{2}\left(p_x^2 + p_y^2 - \frac{n_0^2 R_0^2}{(R_0 + x^2 + y^2)^2}\right). \tag{18}$$

Figure 5 shows a ray trace for the Maxwell fish-eye lens with $n_0 = 2$, meaning that no refraction will take place at the lens surface when it is immersed in air. Examining the inset, we see once again that the velocity Verlet method focuses closest to the exact solution, followed by RK2, RK4 and Ruth's methods, with the standard Euler method's lack of accuracy also becoming more apparent when applied to the Maxwell fish-eye.

In Figure 6, the error of each method appears to decrease exponentially with a reduction in step size. The velocity Verlet method is once again a notable exception to this trend, offering a reduction in error of almost an order of magnitude when compared with the RK2 method. For $\Delta t < 5 \times 10^{-2}$, any differences between RK4 and Ruth's methods are virtually indistinguishable.

Considering the median computation times presented in Figure 7, we see a substantial increase in the time required to ray trace Maxwell's fish-eye for all methods with $\Delta t < 10^{-4}$ when compared with the Lüneburg lens. Again, the velocity Verlet method renders Ruth's method and RK4 redundant, being not only more accurate than them both, but also appreciably faster.

Conclusion

This work emphasises the value of symplectic ray tracing techniques in GRIN media, with the velocity Verlet method showing particular promising due to its disproportionately low error. Results presented here make a strong case for testing other symplectic methods with Lüneburg and Maxwell fish-eye lenses in addition to other GRIN optics for which analytical ray traces do not exist. However, symplectic ray tracing methods will need to account for chromatic effects before being capable of fully characterising any GRIN element. While symplectic numerical methods find an obvious application in optical design, they may also reduce the computational cost of nonlinear GPU ray tracing and other techniques used to render digital images.

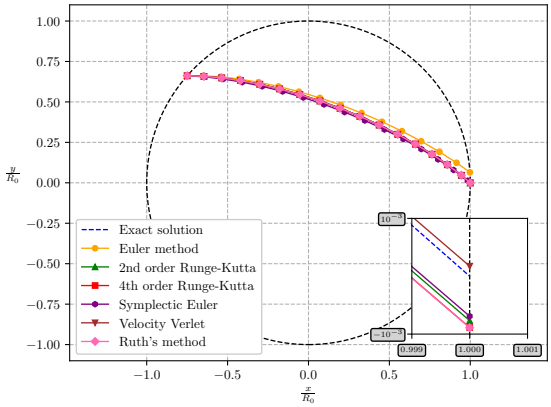

Figure 2. *Numerical ray trace through a Lüneburg lens of radius R_0 with $\Delta t = 0.10$ and initial conditions: $x_0 = -0.75R_0$, $y_0 = \sqrt{1-x_0^2}$, $p_{x_0} = 1$, $p_{y_0} = 0$.*

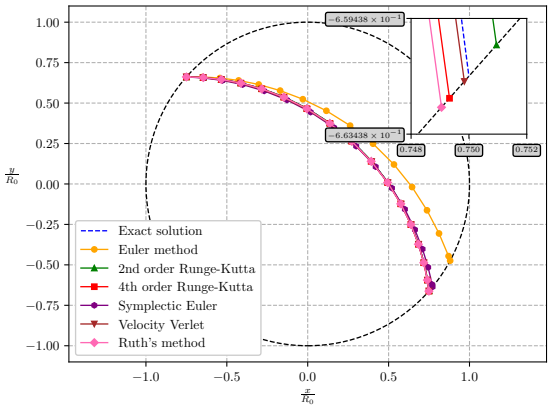

Figure 5. *Numerical ray trace through a Maxwell fish-eye lens with $n_0 = 2$. All other parameters and initial conditions are identical to those in Figure 2.*

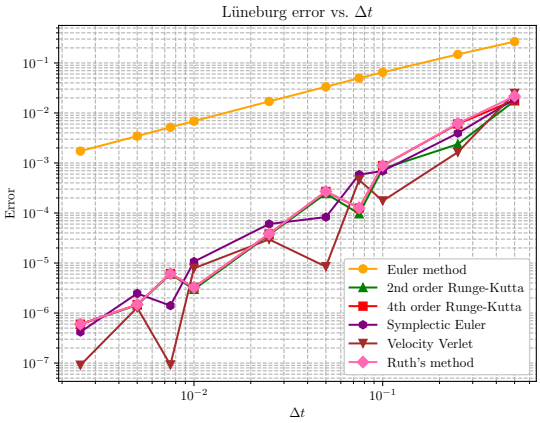

Figure 3. *Error in ray tracing the Lüneburg lens for a variety of step sizes. The error is defined as the distance between the exact and numerical focus along the lens perimeter expressed as a fraction of the lens circumference.*

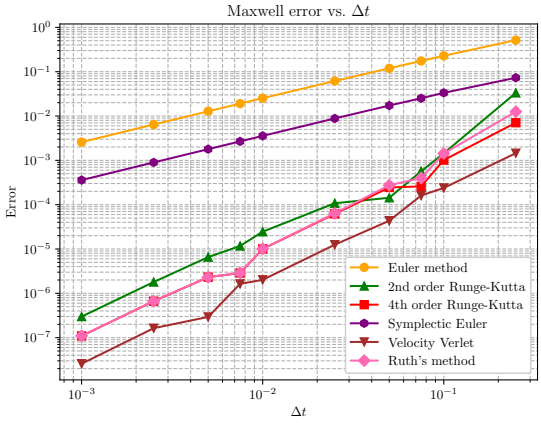

Figure 6. *Error in ray tracing Maxwell's fish-eye lens for each method.*

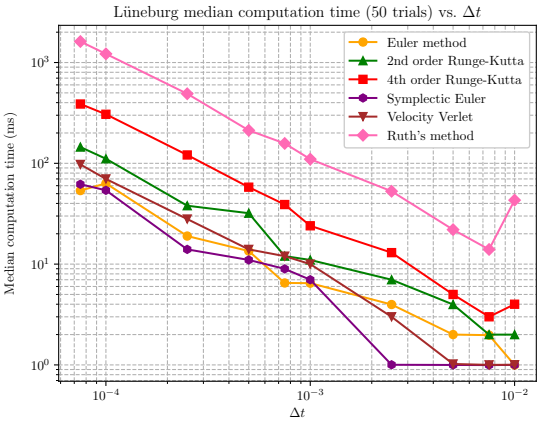

Figure 4. *Median computation time required by each method to ray trace the Lüneburg lens. 50 trials were used to calculate each median time.*

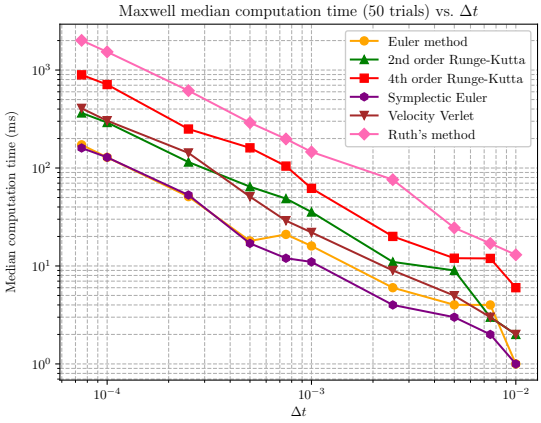

Figure 7. *Median computation time required to ray trace Maxwell's fish-eye lens. As in Figure 4, 50 trials were used to calculate each median time.*

References

[1] J. Babington. “Freeform aberrations in phase space: an example”. In: *JOSA A* 34.6 (2017), pp. 1045–1053.

[2] J. Babington. “Phase space aberrations in freeform and gradient index imaging systems”. In: *Optical Engineering* 57.10 (2018), pp. 105106–105106.

[3] S.H. Badri and M.M. Gilarlue. “Ultrashort waveguide tapers based on Lüneburg lens”. In: *Journal of Optics* 21.12 (2019), p. 125802.

[4] H.A. Buchdahl. *An Introduction to Hamiltonian Optics*. Courier Corporation, 1993.

[5] D. Donnelly and E. Rogers. “Symplectic integrators: an introduction”. In: *American Journal of Physics* 73.10 (2005), pp. 938–945.

[6] K. Feng and D. Wang. “Variations on a theme by Euler”. In: *Journal of Computational Mathematics* (1998), pp. 97–106.

[7] E. Forest and R.D. Ruth. “Fourth-order symplectic integration”. In: *Physica D: Nonlinear Phenomena* 43.1 (1990), pp. 105–117.

[8] H. Goldstein, C. Poole, and J. Safko. *Classical Mechanics*. American Association of Physics Teachers, 2002.

[9] D.J. Griffiths and D.F. Schroeter. *Introduction to Quantum Mechanics*. Cambridge University Press, 2018.

[10] E. Hairer, C. Lubich, and G. Wanner. *Geometric Numerical Integration: structure-preserving algorithms for ordinary differential equations*. Springer, 2006.

[11] E. Hairer and G. Wanner. “Euler methods, explicit, implicit, symplectic”. In: *Encyclopedia of Applied and Computational Mathematics* (2015), pp. 451–455.

[12] W.R. Hamilton. *On a General Method in Dynamics*. Richard Taylor, 1834.

[13] W.R. Hamilton. “Theory of systems of rays”. In: *The Transactions of the Royal Irish Academy* (1828), pp. 69–174.

[14] V. Lakshminarayanan, A. Ghatak, and K. Thyagarajan. *Lagrangian Optics*. Springer Science & Business Media, 2002.

[15] W. Liu et al. “Manipulating light trace in a gradient-refractive-index medium: a Lagrangian optics method”. In: *Optics Express* 27.4 (2019), pp. 4714–4726.

[16] R.K. Lüneburg. *Mathematical Theory of Optics*. University of California Press, 1966.

[17] J.C. Maxwell. *The Scientific Papers of James Clerk Maxwell*. Vol. 2. University Press, 1890.

[18] R. McLachlan. “Symplectic integration of Hamiltonian wave equations”. In: *Numerische Mathematik* 66 (1993), pp. 465–492.

[19] E. Merchand. *Gradient Index Optics*. Elsevier, 2012.

[20] J.M. Nichols. “Approximate solutions for propagating light beams in a material with quadratic, exponential, and quartic transverse refractive index profiles”. In: *Journal of Optics* 22.4 (2020), p. 045601.

[21] H. Ohno and T. Usui. “Gradient-index dark hole based on conformal mapping with etendue conservation”. In: *Optics Express* 27.13 (2019), pp. 18493–18507.

[22] A.J. Parfitt, J.S. Kot, and G.L. James. “The Lüneburg lens as a radio telescope element”. In: *IEEE Antennas and Propagation Society International Symposium. Transmitting Waves of Progress to the Next Millennium. 2000 Digest. Held in conjunction with: USNC/URSI National Radio Science Meeting (C*. Vol. 1. IEEE. 2000, pp. 170–173.

[23] Y.J. Park and W. Wiesbeck. “Offset cylindrical reflector antenna fed by a parallel-plate Lüneburg lens for automotive radar applications in millimeter-wave”. In: *IEEE Transactions on Antennas and Propagation* 51.9 (2003), pp. 2481–2483.

[24] R.J. Pegis. “I. The modern development of Hamiltonian optics”. In: *Progress in Optics*. Vol. 1. Elsevier, 1961, pp. 1–29.

[25] A.A. Rangwala, A.M. Ghodgaonkar, and R.D. Tewari. “Paraxial ray tracing in inhomogeneous optical media”. In: *Optical Engineering* 37.3 (1998), pp. 1025–1032.

[26] J.M. Rebordao and M. Grosmann. “Exact Solutions Of Eikonal Equation And Their Relation To Hamilton Characteristic Functions”. In: *Optical System Design, Analysis, and Production*. Vol. 399. SPIE. 1983, pp. 178–185.

[27] T.R. Satoh. “Symplectic ray tracing: a new approach to nonlinear ray tracing by using Hamiltonian dynamics”. In: *Visualization and Data Analysis 2003*. Vol. 5009. SPIE. 2003, pp. 277–285.

[28] J.L. Synge. *Geometrical Optics: an introduction to Hamilton’s method*. Cambridge University Press, 1937. ISBN: 9780521065900.

[29] A. Torre. *Linear Ray and Wave Optics in Phase Space: bridging ray and wave optics via the Wigner phase-space picture*. Elsevier, 2005.

[30] K.B. Wolf. *Geometric Optics on Phase Space*. Springer Science & Business Media, 2004.

[31] H. Yoshida. “Construction of higher order symplectic integrators”. In: *Physics Letters A* 150.5-7 (1990), pp. 262–268.

[32] L. Zhang et al. “Design of silicon-based integrated gradient index lens”. In: *Journal of Nanophotonics* 14.4 (2020), pp. 046005–046005.

Author Biography

Ben McKeon *is a graduate student at the University of Galway under the supervision of Dr. Alexander Goncharov. He received a BSc. in Mathematics and Physics from the University of Limerick in 2021. Since then, his work has focused on optics. Specifically, he is investigating computationally efficient ways to simulate and characterise optical properties of gradient-index media for use in imaging systems.*

Alexander Goncharov *is primarily interested in the optical design of imaging systems for astronomy, ophthalmology and consumer devices. During his PhD studies, he worked on telescope optics and new concepts in astronomical adaptive optics, wave-front sensing and reconstruction. Currently, his research is in vision science including eye modelling, eye characterisation using new ophthalmic instruments and customisation of contact lenses and intraocular lenses for vision enhancement.*